Behavior of Pyrene End-Labeled Poly(dimethylsiloxane) Polymer Tails in Mixtures of 1-Butyl-3-methylimidazolium Bis(trifluoromethyl)sulfonylimide and Toluene

Wendy E. Gardinier,[†] Gary A. Baker,[‡,§] Sheila N. Baker,[‡] and Frank V. Bright*[,†]

Department of Chemistry, Natural Sciences Complex, University at Buffalo, The State University of New York, Buffalo, New York 14260-3000, and Chemistry Division, Structural Inorganic Chemistry (C-SIC), MS J514, Los Alamos National Laboratory, Los Alamos, New Mexico 87545

Received June 21, 2005; Revised Manuscript Received August 2, 2005

ABSTRACT: We report on the steady-state and time-resolved fluorescence of a linear poly(dimethylsiloxane) polymer that is end-labeled with pyrene (Py-PDMS-Py, $M_n = 3100$, $M_w/M_n = 1.07$) when it is dissolved at low concentration in an ionic liquid,1-butyl-3-methylimidazolium bis(trifluoromethyl)-sulfonylimide ([C_4mim][Tf_2N]), as a function of temperature and added cosolvent (toluene). Toluene is a good solvent for PDMS. The Py-PDMS-Py behavior in [C_4mim][Tf_2N]/toluene is reminiscent, in part, of its behavior in liquid MeOH, a poor PDMS solvent. The Py residues are surrounded by a PDMS-rich microenvironment at all toluene loadings (0−50 vol %). No detectable excimer-like emission is seen in pure [C_4mim][Tf_2N] or [C_4mim][Tf_2N]/toluene mixtures until 50 vol % toluene. The Py-PDMS-Py ground state is heterogeneous, containing monomers and preformed dimers prior to photoexcitation. The observed excimer-like emission does not arise from a dynamic excimer. The Py-PDMS-Py time-resolved intensity decay data reveal the presence of at least four emitting species. In the [C_4mim][Tf_2N]/50% toluene mixture the species are (i) a Py monomer in a PDMS-rich microenvironment, (ii) a Py monomer in a microenvironment between pure toluene and pure [C_4mim][Tf_2N], (iii) a static ground-state dimer that has a geometry akin to a classical dynamically formed excimer, and (iv) a ground-state dimer that has the Py residues misaligned in comparison to (iii). Steady-state fluorescence anisotropy experiments are not consistent with the formation of rigid aggregates (i.e., (Py-PDMS-Py)$_n$); results are consistent with Py residues and PDMS segments of individual Py-PDMS-Py molecules reorienting in a correlated manner.

Introduction

The term ionic liquid (IL) describes a broad class of low-melting semiorganic salts or salt mixtures with an appreciable liquid range.[1−3] There is consensus that a salt must melt at or below 373 K to qualify as an IL. The inherent flexibility afforded by pairing different cations with a growing number of anions provides researchers the potential to fine-tune melting point, water and cosolvent miscibility, viscosity, polarity, acid/base character, and coordinating ability.[1−3] Conservative estimates of the number of practical ILs that can be easily prepared from relatively inexpensive materials reach the tens of thousands; however, there are more than 10 trillion theoretical combinations.

Over the years, ILs have been explored as replacements for traditional molecular liquids (MLs).[1−3] The main attraction of ILs center on their ability to dissolve a wide variety of inorganic and organic solutes, their low volatility, their high thermal stability, and their tunable physicochemical properties. More recently, ILs have been investigated as solvents for performing free-radical, transition-metal-mediated living free-radical, charge-transfer, cationic, and thermal polymerizations.[4−8] How do polymers behave in an IL?

In this paper we investigate the tail segments of a linear poly(dimethylsiloxane) polymer ($M_n = 3100$, $M_w/M_n = 1.07$) that has been end-labeled with pyrene (Py-PDMS-Py, Figure 1A)[9] when it is dissolved in pure 1-butyl-3-methylimidazolium bis(trifluoromethyl)sulfonylimide ([C_4mim][Tf_2N], Figure 1A) and mixtures of [C_4mim][Tf_2N] and toluene between 293 and 373 K. In pure toluene the Py-PDMS-Py tail−tail cyclization dynamics follow a classic Birks model (Figure 1B); however, one can modulate this behavior under certain circumstances in MLs.[9] Bright and co-workers have demonstrated that cosolvents and temperature can alter an IL's properties (i.e., viscosity, density, and water miscibility) and solute solvation.[10] In related work, Baker et al.[11] have reported on the temperature-dependent behavior of short chain flexible 1,*n*-bis(pyrenyl)alkanes dissolved in pure *N*-butyl-*N*-methylpyrrolidinium bis(trifluoromethyl)sulfonylimide ([C_4mpy][Tf_2N]). The current study is the first to investigate the behavior of polymer tail segments dissolved in pure ILs and IL/cosolvent mixtures. The aim is to determine how the local microenvironment surrounding the tail segments is influenced by an IL, cosolvent, and temperature.

Theory Section

Figure 1B presents a simplified energy-level diagram describing the behavior of isolated flexible molecules like Py-PDMS-Py undergoing intramolecular excimer formation (i.e., tail−tail cyclization) within a Birks framework.[12] This model suffices to describe the behavior of molecules like Py-PDMS-Py in a good PDMS solvent like toluene.[9,12b,c] Here, monomeric Py-PDMS-Py molecules (1) are photoexcited ($h\nu_{ex}$) to produce an excited-state (*) monomer (2). In this scheme, the excited-state monomers have two possible fates. They can deexcite back to the ground state with overall rate k_M. In a

† University at Buffalo.
‡ Los Alamos National Laboratory.
§ Current address: Chemical Sciences Division, Oak Ridge National Laboratory, P.O. Box 2008, Oak Ridge, TN 37831-6110.
* To whom all correspondence should be addressed: Ph 716-645-6800 ext 2162; Fax 716-645-6963; e-mail chefvb@acsu.buffalo.edu.

10.1021/ma051313n CCC: $30.25
Published on Web 09/03/2005

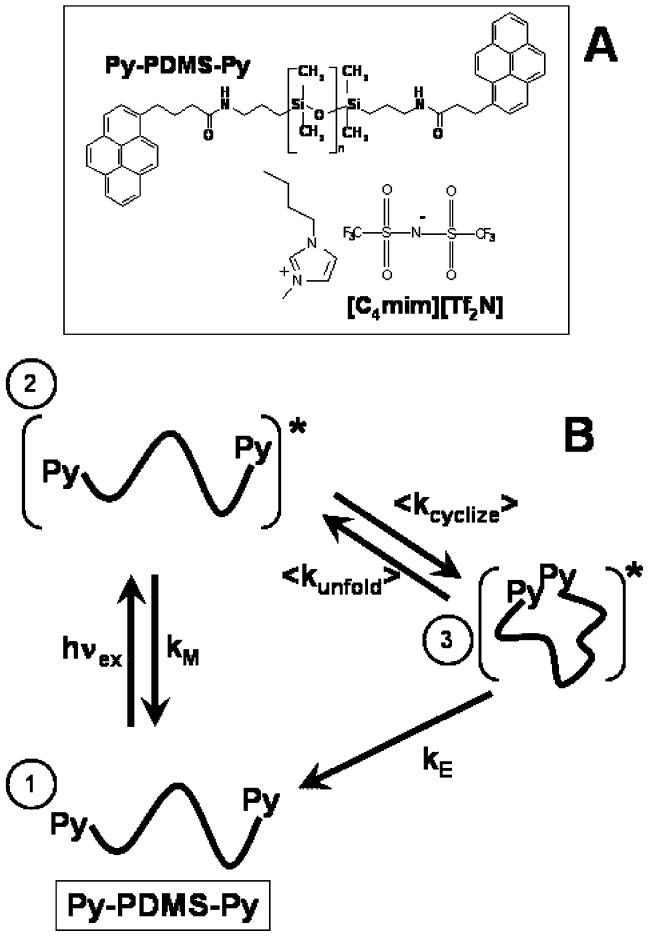

Figure 1. Chemical structure of Py-PDMS-Py and $[C_4mim][Tf_2N]$ (panel A) and simplified schematic describing the photophysics of Py-PDMS-Py within a Birks framework (panel B). Rate coefficients (all unimolecular) are as follows: k_M, excited-state monomer to ground-state monomer relaxation; k_E, excited-state excimer to ground-state monomer relaxation; $\langle k_{cyclize}\rangle$, excited-state intramolecular tail−tail cyclization; and $\langle k_{unfold}\rangle$, excited-state tail−tail unfolding.

second pathway, the tail residues on the excited-state monomer can cyclize intramolecularly with rate $\langle k_{cyclize}\rangle$, forming an intramolecular excited-state (*) excimer (3). The so-formed excimers (dynamically formed excited-state dimers) also have two possible fates. They can unfold with rate $\langle k_{unfold}\rangle$ to re-form the excited-state monomer, or they can deexcite back to the ground-state monomer with overall rate k_E. (Note: $\langle\ \rangle$ is used with some of the rate terms to remind the reader that all oligomers and polymers exhibit some degree of polydispersity.)

Figure 1B predicts[12] that the monomer time-resolved fluorescence intensity ($I_M(t)$) will decay as the sum of two exponentials and the excimer time-resolved emission intensity ($I_E(t)$) will decay as the difference of two exponentials:

$$I_M(t) = a_1 \exp(-\lambda_1 t) + a_2 \exp(-\lambda_2 t) \quad (1)$$

$$I_E(t) = a_3 \exp(-\lambda_3 t) - a_4 \exp(-\lambda_4 t) \quad (2)$$

with the following constraints: $\lambda_1 = \lambda_3$, $\lambda_2 = \lambda_4$, and $a_4/a_3 = 1$. If Figure 1B describes the system photophysics, one can recover all the kinetic terms from the apparent decay times.[12] If the system photophysics are more complex than is portrayed by Figure 1B, more complex models can sometimes be utilized.

In the current work, we use a global analysis strategy[13] by acquiring time correlated single photon counting fluorescence data at two or more emission wavelengths across the Py-PDMS-Py emission spectrum, and we analyze these data sets simultaneously to recover the preexponential terms and decay times.

In dilute solution one can study aggregation by recording the steady-state fluorescence anisotropy, r:[14,15]

$$r = (I_{||} - GI_{\perp})/(I_{||} + 2GI_{\perp}) \quad (3)$$

In this expression $I_{||}$ and $I_{\perp}$ represent the parallel and perpendicular components of the polarized fluorescence intensity when the sample is excited with vertical polarized electromagnetic radiation.[14,15] G is an instrumental factor that corrects for differing sensitivities of the sample cell windows, lenses, optical filters, gratings, and detector envelope to the emission polarization. In the simplest case of isotropic rotational reorientation, r is given by the Perrin equation:[14]

$$r = r_0/[1 + (\tau/\phi)] \quad (4)$$

where r_0 is the fluorophore limiting anisotropy, τ is the fluorophore excited-state lifetime, and ϕ is the fluorophore rotational reorientation time. r_0 is measured for the fluorophore in the absence of rotational diffusion and is determined experimentally in vitrified solution (e.g., glycerol at 223 K). Under our experimental conditions, the 1-pyrenyl (Py) residue r_0 value is 0.20 ± 0.03.[16]

The Debye−Stokes−Einstein expression[14a,b]

$$\phi = \eta V/RT \quad (5)$$

provides a link between ϕ and the volume, V, of the rotating fluorophore along with anything attached *to* the fluorophore (e.g., a tether or an aggregate).[14,15] R and T are the gas constant and Kelvin temperature, respectively. A variation of eq 5 is often used to estimate the rotational reorientation time for "globular" species:[14a,b]

$$\phi = \eta M/RT(v_s + s) \quad (6)$$

In this expression, M is the molecular weight of the rotating body/entity, v_s is its specific volume, and s is the solvation (grams of solvent/gram of solute).

Experimental Section

Chemicals and Reagents. The following chemicals were used as received: toluene (Sigma-Aldrich, 99.8%, anhydrous), ethyl acetate (Aldrich, 99.8%, anhydrous), lithium bis(trifluoromethanesulfonyl)imide (3M Specialty Chemicals), NH_2-PDMS-NH_2 (United Chemical Technologies), 1-pyrenebutanoic acid succinimidyl ester (Molecular Probes), and 1-ethylpyrene (1-EP, Molecular Probes). 1-Methylimidazole (Aldrich, ≥99%) and 1-bromobutane (Aldrich, ReagentPlus ≥99%) were redistilled immediately prior to use.

Synthesis of 1-Butyl-3-methylimidazolium Bis(trifluoromethanesulfonyl)imide. The synthesis of 1-butyl-3-methylimidazolium bis(trifluoromethanesulfonyl)imide ($[C_4mim][Tf_2N]$) followed a modification of a method reported by Baker et al.[17] Under dry N_2 on a Schlenk line, a 20% molar excess of freshly distilled 1-bromobutane (39.2 mL, 0.365 mol) was added dropwise over 30 min to stirring 1-methylimidazole (24.2 mL, 0.304 mol) in a 250 mL round-bottom flask at 273 K. The flask was covered with aluminum foil, and the reaction proceeded at room temperature for 96 h. After removing volatiles by rotary evaporation, the mixture was seeded with solid 1-butyl-3-methylimidazolium, $[C_4mim]Br$, frequently resulting in rapid solidification within 1−2 h. The resulting

white to off-white precipitate was then washed with cold ethyl acetate (5 × 25 mL) followed by solvent removal on a rotary evaporator and overnight drying in a vacuum oven at 313 K to afford [C_4mim]Br in about 90% yield. ^{1}H NMR (400 MHz, acetone-d_6, δ/ppm relative to TMS): 10.31 (s, 1H), 7.98 (s, 1H), 7.89 (s, 1H), 4.46 (t, 2H, J = 7.2 Hz), 4.11 (s, 3H), 1.93 (m, 2H, J = 7.2 Hz), 1.38 (m, 2H, J = 7.2 Hz), 0.94 (t, 3H, J = 7.2 Hz).

For spectroscopic applications, the [C_4mim]Br must be further purified prior to metathesis. Toward this end, [C_4mpy]-Br was dissolved at ca. 0.5 g/mL in 18.2 MΩ·cm doubly distilled, deionized water and refluxed overnight with decolorizing carbon. The charcoal was subsequently removed by centrifugation at 5000 rpm for 15 min followed by decanting into a fresh Eppendorf tube. This was repeated once followed by filtration through a 0.45 μm nylon syringe filter. The resulting solution was flash frozen in liquid nitrogen and lyophilized to dryness over 48 h. Metathesis was performed by mixing, in a single addition, a 0.5 mg/mL aqueous solution of the so-purified [C_4mim]Br and lithium bis(trifluoromethanesulfonyl)imide (1.05 equiv) dissolved in a minimal amount of deionized water. The mixture was vigorously stirred overnight at room temperature whereupon the dense lower ionic liquid phase was collected using a separatory funnel and repeatedly extracted with water using at least 15 equivalent volumes. The [C_4mim][Tf_2N] was then dried at room temperature under high vacuum (10^{-4} bar) for 96 h to afford the color-free "spec-grade" IL. The water content in the final IL was less than 150 ppm as determined from a Karl Fischer conductometric titration. ^{1}H NMR (400 MHz, acetone-d_6, δ/ppm relative to TMS): 9.04 (s, 1H), 7.78 (s, 1H), 7.72 (s, 1H), 4.37 (t, 2H, J = 7.2 Hz), 4.07 (s, 3H), 1.93 (m, 2H, J = 7.2 Hz), 1.39 (m, 2H, J = 7.2 Hz), 0.94 (t, 3H, J = 7.2 Hz).

[C_4mim][Tf_2N] was prepared at Los Alamos National Laboratories and packaged under argon in Sure/Seal bottles. To avoid the sorption of environmental moisture, all [C_4mim]-[Tf_2N] storage and transfers were performed within an argon-purged drybox (Vacuum Atmospheres Co., model no. HE-43-2).

Synthesis of Py-PDMS-Py and PDMS-Py.[9a] NH_2-PDMS-NH_2 or PDMS-NH_2 were reacted in anhydrous toluene at room temperature with a 10-fold molar excess of 1-pyrenebutanoic acid succinimidyl ester for 24 h with stirring in the dark under N_2 or argon atmospheres. The desired products were isolated by gel permeation chromatography, and their structures were confirmed by matrix-assisted laser desorption/ionization time-of-flight mass spectrometry. Py-PDMS-Py had the following characteristics: M_n = 3100; M_w/M_n = 1.07. There was no significant (<0.3%) single-labeled product in the Py-PDMS-Py samples. The PDMS-Py polymer had the following characteristics: M_n = 2800; M_w/M_n = 1.09.

Instrumentation. All electronic absorbance measurements were performed by using Milton-Roy model 1201 or HP model 8452A UV−vis spectrophotometers.

Viscosities were determined by using a cone plate viscometer (Brookfield DV-II+). The viscometer sample temperature was regulated to ±1 K with a temperature bath (Brookfield TC-602). The viscometer was housed within the argon-purged drybox.

Steady-state excitation and emission spectra were recorded with an SLM-AMINCO model 48000 MHF spectrofluorometer. The excitation source was a 450 W xenon arc lamp. Wavelength selectors were single grating monochromators. The spectral band-pass for a given scan was 1 nm. All spectra were corrected by using appropriate blanks. The blank contribution to the total emission was always <5%.

Steady-state anisotropy measurements were also performed by using the SLM-AMINCO model 48000 MHF spectrofluorometer. Samples were excited with vertically polarized light at 325 nm. The pyrene monomer fluorescence was monitored using a 380 nm band-pass filter (Oriel). All data were appropriately blank and G-factor corrected.

All time-resolved fluorescence experiments were carried out by using an IBH model 5000 W SAFE time-correlated single photon counting fluorescence lifetime instrument. An N_2-filled coaxial flash lamp served as the excitation source. The flash lamp repetition rate was maintained at 40 kHz. Single grating monochromators were used for wavelength selection. The excitation wavelength was adjusted to 337 nm (band-pass of 8 or 16 nm). To avoid pulse pileup, the count rate at each detector was always <2% of the flash lamp repetition rate. The instrument response function (IRF) and the time-resolved fluorescence intensity decay traces (under magic angle polarization conditions)[18] were simultaneously recorded. In a typical experiment we acquired the IRF plus the time-resolved intensity decay at four emission wavelengths distributed across the emission spectrum. In some experiments we recorded time-resolved intensity decay data at up to 14 emission wavelengths. The typical time resolution for an experiment was 0.47 ns/channel, and we used 1024 channels within the multichannel analyzer (MCA). A dilute solution of 9-cyanoanthracene in ethanol was regularly used as a reference lifetime standard (τ_{ref} = 11.73 ns)[19] to confirm proper instrument operation. All experiments were conducted until there were at least 10^4 counts in the peak MCA channel. The time-resolved intensity decay data were analyzed using Globals WE (Globals Unlimited), a commercially available global analysis software package.

Sample Preparation. O_2 quenching can seriously bias fluorescence experiments. To avoid this problem and any problems with adventitious water, we prepared all of our samples within an argon-purged drybox. All samples for spectroscopic investigation were prepared within 1 cm^2 fused silica freeze−pump−thaw cuvettes. Five freeze−pump−thaw cycles were used to remove O_2. The Py-PDMS-Py, Py-PDMS, and 1-EP concentrations were <20 μM.

The sample temperature was controlled to within 0.1 K by using a Neslab model RTE-111 refrigerated bath circulator.

All experiments were carried out from 293 K to at least 353 K, but most were run up to 373 K. There was no evidence of hysteresis. To ensure equilibration following a temperature change, excitation and emission spectra were recorded 20−30 min after each temperature change. Replicate spectra were always recorded to ensure that we were at equilibrium and to provide a statistical measure of the measurement imprecision.

Reporting. All results are reported as the measured mean and the standard deviation from at least five separate experiments.

Results and Discussion

Steady-State Fluorescence. In a ML pyrene excites between 310 and 350 nm and it fluoresces between 370 and 550 nm. The pyrene monomer emits primarily between 370 and 420 nm, and excimer emission appears between 440 and 550 nm. Figure 2 presents typical steady-state emission spectra for Py-PDMS-Py in [C_4-mim][Tf_2N] at 293 (—), 323 (· · ·), and 353 K (- - -) in the presence of 0 (panel A), 1 (panel B), 10 (panel C), and 50% (v/v) toluene (panel D). All spectra have been normalized to the highest energy peak in the monomer portion of the spectrum. The monomer emission can be clearly observed between 370 and 430 nm in all samples. The excimer-like emission is typically seen in the 440−550 nm region. There is no evidence of excimer emission from 1-EP or Py-PDMS, the model monomer compounds, at the same fluorophore concentrations and experimental conditions (results not shown).

The excimer to monomer emission intensity ratio (E/M, = I_{480}/I_{376}) provides a qualitative measure of relative chain conformation, system dynamics, and/or intermolecular chain interactions.[9,12] Figure 3 summarizes the Py-PDMS-Py E/M as a function of solvent composition and temperature. There is very little excimer-like emission from the Py-PDMS-Py in pure [C_4mim][Tf_2N] or the [C_4mim][Tf_2N]/toluene samples that contain up to 10% toluene. The E/M for these samples increases slightly with increasing temperature. In the [C_4mim]-

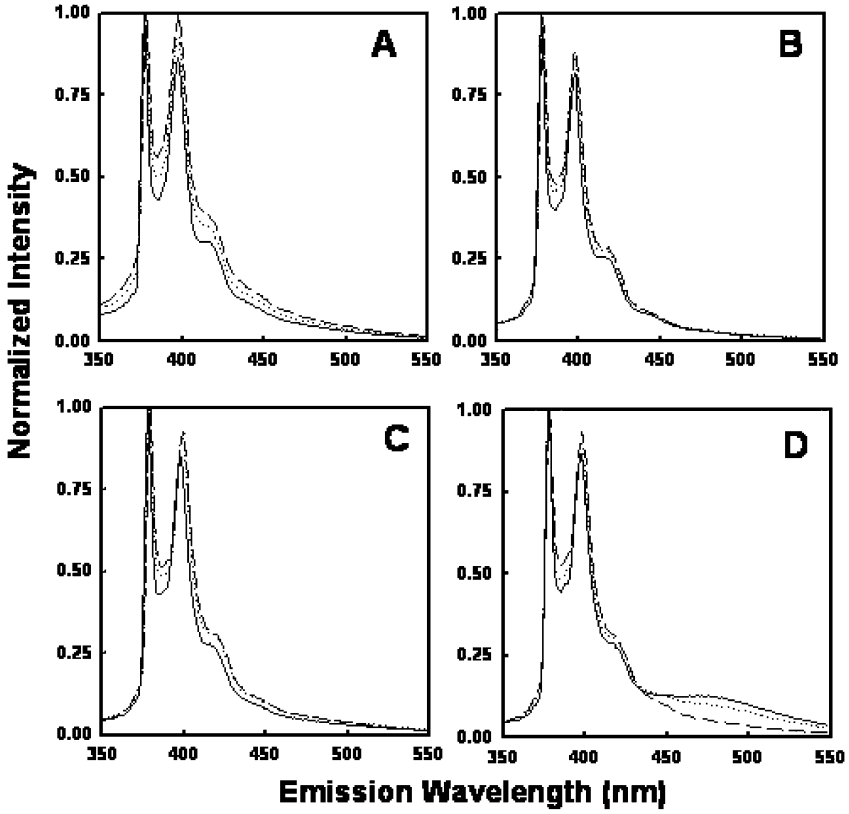

Figure 2. Effects of temperature and composition on the Py-PDMS-Py steady-state emission spectra in [C_4mim][Tf_2N]: (panel A) pure [C4mim][Tf_2N]; (panel B) [C_4mim][Tf_2N]/1% toluene; (panel C) [C_4mim][Tf_2N]/10% toluene; (panel D) [C_4mim][Tf_2N]/50% toluene. In each panel spectra are shown at 293 (—), 323 (· · ·), and 353 K (- - -).

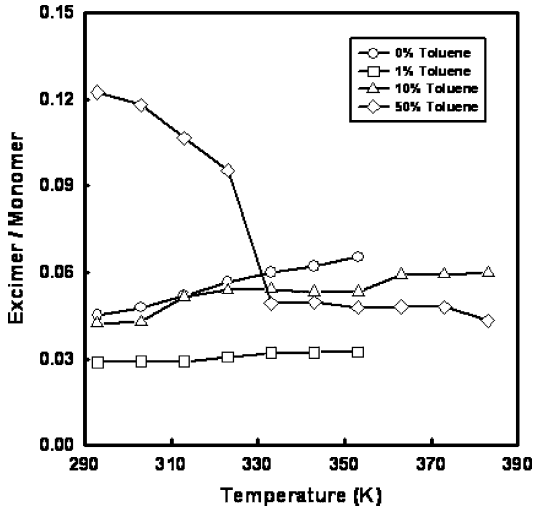

Figure 3. Effects of temperature and added toluene on the Py-PDMS-Py excimer-to-monomer intensity ratio (E/M, = I_{480}/I_{376}) in the IL phase. λ_{ex} = 325 nm. Excitation band-pass = 16 nm. Emission band-pass = 1 nm. The uncertainty in each datum is smaller than the size of each point.

[Tf_2N]/50% toluene samples at 293 K, we note a significant increase in the E/M in comparison to the other [C_4mim][Tf_2N]/toluene mixtures at the same temperature (see Figure 2D also). As we increase the solution temperature, the Py-PDMS-Py E/M from the sample that contains 50% toluene decreases, approaching values near the [C_4mim][Tf_2N]/10% toluene samples above 350 K. There are several possible explanations for this behavior.

We began to investigate these result by exploring the [C_4mim][Tf_2N]/toluene mixture phase behavior. Samples that contained 10% or less toluene remained visually homogeneous over the temperature range investigated (i.e., 293−383 K). As shown in Figure 4A, the [C_4mim][Tf_2N]/50% toluene sample also remained homogeneous between 293 and 323 K; however, the solution split into two discrete phases above 323 K. The less dense, toluene-rich phase is at the top. Thus, as we increase the [C_4mim][Tf_2N]/50% toluene mixture temperature, the concentration of toluene that is dissolved in the [C_4mim][Tf_2N] phase decreases.

We also investigated the temperature-dependent viscosity of the IL phase in pure [C_4mim][Tf_2N] and the [C_4mim][Tf_2N]/50% toluene mixture (Figure 4B). If solvent viscosity alone were the reason for the observed E/M behavior, E/M would scale inversely with viscosity. Although there is clearly more excimer-like emission in the less viscous [C_4mim][Tf_2N]/50% toluene mixture at 293 K, the E/M values for Py-PDMS-Py in [C_4mim][Tf_2N]/50% toluene are *not* 5−6 times larger than those for Py-PDMS-Py dissolved in pure [C_4mim][Tf_2N]. This result indicates that the behavior seen in Figure 3 is not solely due to differences in solvent viscosity. In addition, above 350 K, the two IL solutions (pure IL and IL + toluene) exhibit nearly equal viscosities. The recovered activation energies for viscous flow ($E_{a,\eta}$) are 31.6 ± 0.3, 11.0 ± 0.1, and 8.9 ± 0.2 kJ/mol[20] for pure [C_4mim][Tf_2N], [C_4mim][Tf_2N]/50% toluene, and toluene, respectively. The $E_{a,\eta}$ for the pure IL is nearly 3 times that of the IL with 50 vol % toluene, which is close to the value for pure toluene.

We next questioned the effect of solvent composition and temperature on the local microenvironment that surrounds the Py residue within the Py-PDMS-Py molecules in pure [C_4mim][Tf_2N] and the [C_4mim][Tf_2N]/

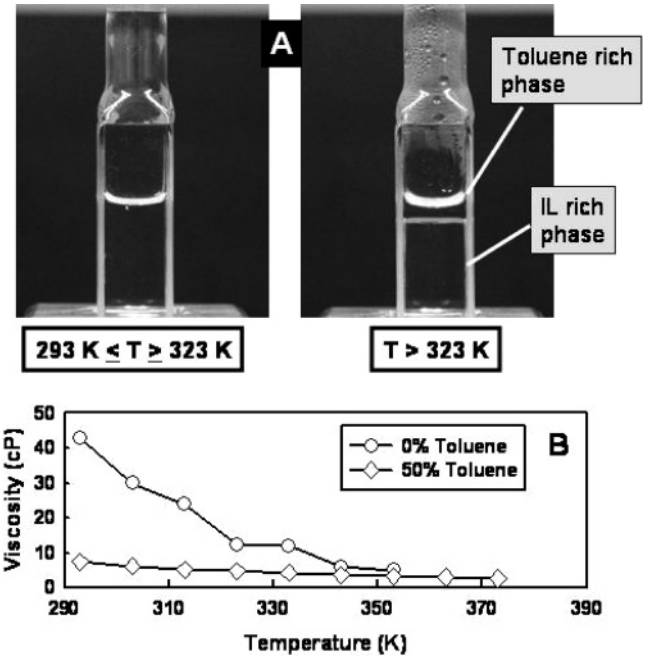

Figure 4. Phase behavior and viscosity dependence of [C_4mim][Tf_2N] and [C_4mim][Tf_2N]/50% toluene: (panel A) photographs of [C_4mim][Tf_2N]/50% toluene mixture between 293 and 323 K (left, one phase) and above 323 K (right, two phases); (panel B) temperature-dependent viscosity profiles for pure [C_4mim][Tf_2N] and [C_4mim][Tf_2N]/50% toluene. The uncertainty in each datum is smaller than the size of each point.

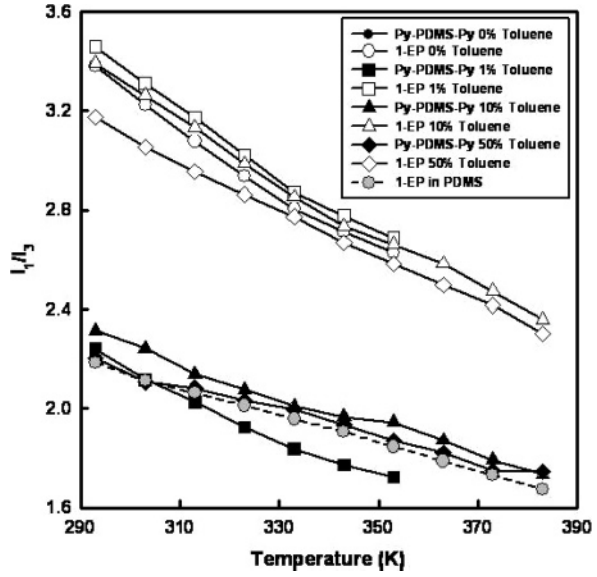

Figure 5. Effects of composition and temperature on the Py residue I_1/I_3 in 1-EP and Py-PDMS-Py in pure [C_4mim][Tf_2N] and [C_4mim][Tf_2N]/toluene mixtures. The behavior of Py-PDMS (not shown) parallels Py-PDMS-Py. The uncertainty in each datum is smaller than the size of each point.

toluene mixtures. The local micorenvironment surrounding pyrene molecules can be assessed by recording the intensity ratio of the I_1 to I_3 emission bands.[21,22] Figure 5 summarizes the temperature-dependent I_1/I_3 emission band ratio for 1-EP and Py-PDMS-Py in pure [C_4mim][Tf_2N] and [C_4mim][Tf_2N]/toluene mixtures. (Note: The behavior of Py-PDMS was indistinguishable from Py-PDMS-Py under equivalent conditions.) Although the Py residue's I_1/I_3 is not equivalent to the well-know I_1/I_3 for pyrene molecules,[22] the Py residue's I_1/I_3 is still very sensitive to the physicochemical properties of its local microenvironment. For example, using 1-EP as our benchmark, I_1/I_3 at 308 K ranges from 1.13 $\pm$ 0.01 in pure methyl-terminated PDMS to 2.11 $\pm$ 0.01 in pure amino-terminated PDMS to 3.27 $\pm$ 0.01 in pure methanol. Inspection of the data presented in Figure 5 shows several interesting trends. First, as the temperature increases, I_1/I_3 decreases. This is consistent with predictable changes in the frequency-dependent dielectric response of the system. Second, the 1-EP I_1/I_3 in a given solvent at a given temperature is significantly greater in comparison to the corresponding I_1/I_3 for Py-PDMS-Py in the same solvent system (e.g., at 293 K, the 1-EP I_1/I_3 in pure [C_4mim][Tf_2N] is $\sim$3.4 whereas the Py-PDMS-Py I_1/I_3 in pure [C_4mim][Tf_2N] is $\sim$2.2). These results demonstrate that in the ILs the local microenvironment that surrounds the Py residue (cybotactic region) in Py-PDMS-Py is similar to pure PDMS. That is, the Py residue cybotactic region is enriched in PDMS when the Py-PDMS-Py is dissolved in [C_4mim][Tf_2N]. Together, these results are consistent with the Py residues on Py-PDMS-Py molecules interacting preferentially with the same or other PDMS segments.

It is important to distinguish between dynamic excimers that are formed exclusively during an excited-state reaction and static "dimers" or "higher-order species" (e.g., aggregates) that result from the preassociation of the Py residues in the ground state prior to optical excitation. To address this issue, we acquired a series of emission wavelength-dependent excitation spectra as a function of solvent composition and temperature.[9,23] If the Py-PDMS-Py/[C_4mim][Tf_2N]/toluene system is described by a purely dynamic excimer (e.g., Figure 1B), the normalized excitation spectra will be superimposable and independent of emission wavelength.[9,23] If the emission wavelength-dependent excitation spectra are shifted relative to one another, this indicates the presence of static ground-state dimers/multimers in the polymer system.[9,23] Figure 6 presents a typical series of normalized emission wavelength-dependent excitation spectra for Py-PDMS-Py in pure [C_4mim][Tf_2N] and [C_4mim][Tf_2N]/toluene mixtures at 293 K. Similar spectra were recorded at all other temperatures. The spectra within each panel (solvent composition) are not superimposable. (Note: The corresponding spectra for 1-EP and Py-PDMS are superimposable.) The correlation coefficients for the $I_{376}(\lambda_{ex})$ vs $I_{480}(\lambda_{ex})$ plots[23a] (not shown) are substantially less than unity. However, we note that the correlation coefficient for the $I_{376}(\lambda_{ex})$ vs $I_{480}(\lambda_{ex})$ plots get closer to unity as the added toluene vol % increases (compare Figure 6A to Figure 6D). These results argue that the observed excimer is not formed in a purely dynamical manner in the excited state a la Figure 1B. These results are consistent with a heterogeneous ground state (i.e., some degree of inter- or intramolecular preassociation of the Py residues in the ground state prior to photoexcitation). Thus, the model presented in Figure 1B will not suffice to describe the Py-PDMS-Py photophysics in pure [C_4mim][Tf_2N] and [C_4mim][Tf_2N]/toluene over the solvent composition and temperature range studied.

Time-Resolved Intensity Decay Studies. The steady-state spectroscopy argues that the Py-PDMS-Py ground state is heterogeneous, and the local microenvironment surrounding the Py residues in Py-PDMS-Py in pure [C_4mim][Tf_2N] and [C_4mim][Tf_2N]/toluene

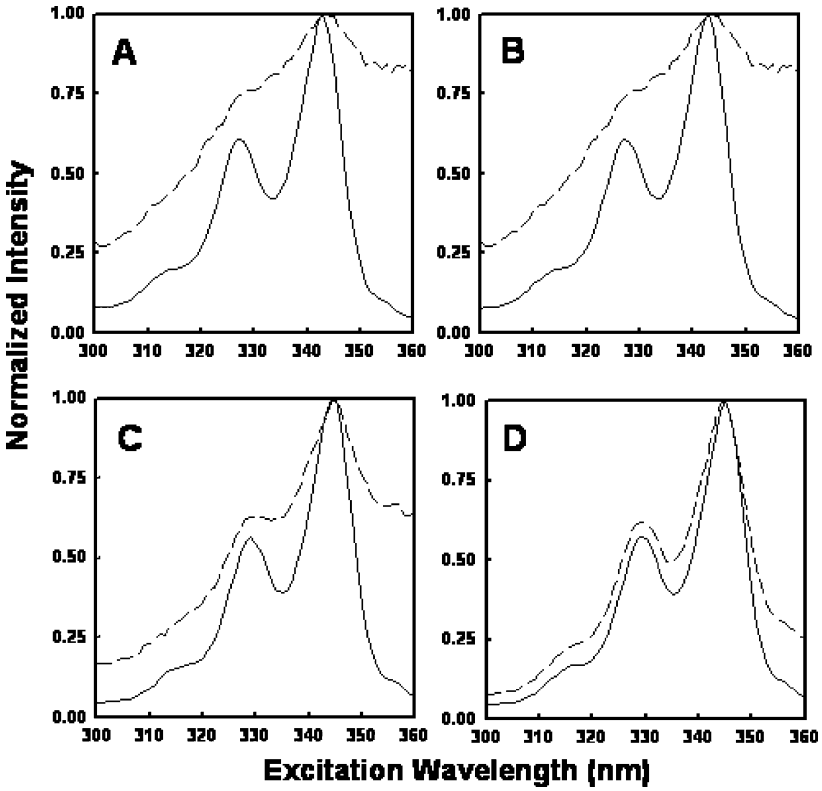

Figure 6. Normalized emission wavelength-dependent fluorescence excitation spectra for Py-PDMS-Py in pure [C_4mim][Tf_2N] and [C_4mim][Tf_2N]/toluene mixtures at 293 K recorded while monitoring the emission at 376 (—) and 480 nm (- - -): (panel A) pure [C_4mim][Tf_2N]; (panel B) [C_4mim][Tf_2N]/1% toluene; (panel C) [C_4mim][Tf_2N]/10% toluene; (panel D) [C_4mim][Tf_2N]/50% toluene. Emission and excitation spectral band-passes were 16 and 1 nm, respectively.

mixtures is rich in PDMS. To explore the system photophysics in more detail, we carried out a series of time-resolved intensity decay experiments on 1-EP and Py-PDMS-Py in pure [C_4mim][Tf_2N] and [C_4mim][Tf_2N]/toluene mixtures. The 1-EP time-resolved intensity decay in pure [C_4mim][Tf_2N] and [C_4mim][Tf_2N]/toluene mixtures between 293 and 393 K is single exponential over at least four lifetimes ($\chi^2_{global} \leq 1.12$). The recovered excited-state fluorescence lifetime (τ) decreases with increasing temperature and follows Arrhenius behavior with an activation energy for thermal quenching ($E_{a,T}$) that is solvent independent (i.e., $E_{a,T}$(pure [C_4mim][Tf_2N]) = 1.8 ± 0.3 kJ/mol, $E_{a,T}$([C_4mim][Tf_2N]/50% toluene) = 1.6 ± 0.3 kJ/mol, and $E_{a,T}$(toluene) = 1.7 ± 0.2 kJ/mol[24]).

On the basis of the steady-state results, we anticipated that the Py-PDMS-Py time-resolved intensity decay results in pure [C_4mim][Tf_2N] and [C_4mim][Tf_2N]/toluene mixtures would be complex. To investigate this system in more detail, we recorded the time-resolved intensity decay traces at up to 14 emission wavelengths distributed across the Py-PDMS-Py emission spectrum, and we used global analysis[13] to determine the best model. (Note: To clarify the presentation that follows, we only present the data and fits at one monomer and one "excimer" emission wavelength (i.e., 376 and 480 nm). However, all 14 time-resolved intensity decay data sets were used during the global analysis.)

On the basis of an analysis of all 14 residual and autocorrelation profiles plus the χ^2_{global}, we conclude that the single-exponential ($\chi^2_{global} = 622$), double-exponential/Birks ($\chi^2_{global} = 14.9$), and triple-exponential models ($\chi^2_{global} = 2.09$) do not describe the Py-PDMS-Py/[C_4mim][Tf_2N] intensity decay data well. Of the models tested, the quadruple exponential decay model ($\chi^2_{global} = 1.10$, Figure 7) describes the Py-PDMS-Py/[C_4mim][Tf_2N] time-resolved intensity decay data best. (Note: We also investigated unimodal and multimodal continuous lifetime distribution models; the fits were not better in comparison to a quadruple exponential decay model.) The quadruple exponential decay model was also the best model for all solvent compositions and temperatures. (Note: In experiments with Py-PDMS, the best fit was a double-exponential model, but there were no negative preexponential terms. This is discussed further below.)

The fluorescence from any fluorophore or mixture of fluorophores is a function of time and emission wavelength.[25] Given this, one can extract the individual kinetic parameters and the corresponding spectra from a heterogeneous population of emissive species, if the species exhibit different spectral profiles and/or excited-state fluorescence intensity decay kinetics.[25] The decay associated spectra (DAS)[25] for Py-PDMS-Py in [C_4mim][Tf_2N]/50% toluene at 293 K are presented in Figure 8. These DAS show that the observed Py-PDMS-Py emission in [C_4mim][Tf_2N]/50% toluene arises from at least four species with apparent excited-state lifetimes of 240 ± 5, 166 ± 2, 28 ± 0.5, and 2 ± 0.4 ns. There are no negative preexponential factors recovered at any wavelength at any composition or temperature studied. (Note: The corresponding results for Py-PDMS are double exponential with decay times of 235 ± 4 and 159 ± 2 ns.) As a benchmark, the excited-state lifetime for 1-EP at 303 K in pure toluene, [C_4mim][Tf_2N], and methyl-terminated PDMS are 190 ± 3, 160 ± 8, and 245 ± 7 ns, respectively.

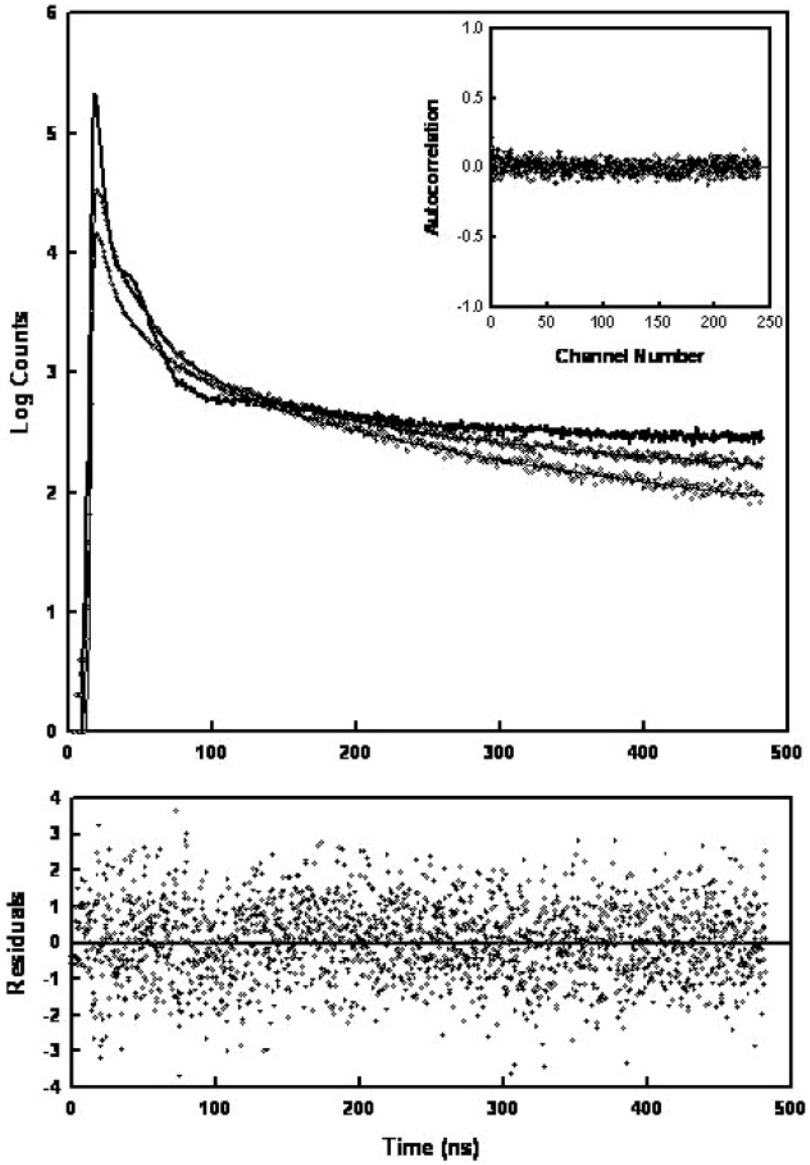

Figure 7. Typical time-correlated single photon counting data, instrument response function (IRF), residuals, and autocorrelation traces for Py-PDMS-Py in pure [C_4mim][Tf_2N]. The monomer and excimer emission were acquired simultaneously at 376 nm (closed circles) and 480 nm (open circles), respectively. Fit (solid curve) to a quadruple exponential decay is shown. $\chi^2_{\text{global}} = 1.10$.

The 240 ns component emits in the monomer region only. This result is consistent with Py residues that are encountering a significant amount of PDMS. The 166 ns component also emits in the monomer region. This result is consistent with Py residues that encounter a microenvironment between pure toluene and pure [C_4-mim][Tf_2N]. The 28 ns component emits in the excimer region only, and its maximum appears near 480 nm. This component is consistent with a static species (e.g., a ground-state dimer) that has classic[12a] dynamically formed excimer geometry.[12a] The 2 ns component also emits in the excimer region only; however, this component's emission spectrum is blue-shifted in comparison to the standard excimer.[12a] These features are consistent with a second type of ground-state dimer/static excimer wherein the Py residues are in close proximity but not aligned like in a traditional excimer.[26] For example, blue-shifted excimers have been observed previously for 16-(1-pyrenyl)hexadecanoic acid and stearic acid Langmuir−Blodgett monolayers,[26a,b] vacuum-deposited films of T-(1-pyrenyl)alkanoic acids,[26c] pyrene-labeled hydroxypropyl cellulose polymers in water,[26d] multilayer films of pyrene-labeled cellulose octadecanoate,[26e] di-1-pyrenyl-substituted organosilanes,[26f] 1,3-dipyrenylpropanes with partial ring overlaps,[26g] and Langmuir−Blodgett films composed of pyrene and stearic acid.[26h] In each of the aforementioned systems an excimer feature is observed to the blue of the traditional excimer, arising from incomplete pyrene ring overlap and/or a symmetrical structure wherein the pyrene/pyrenyl residues are not parallel relative to each other.

Steady-State Fluorescence Anisotropy Studies. Aggregation of the Py-PDMS-Py molecules would result in the highest rotational correlation time values, followed by lower values for nonaggregated Py-PDMS-Py molecules with collapsed PDMS arms. The lowest rotational correlation time values are anticipated for well-solvated, isolated Py-PDMS-Py molecules where there is minimal interaction between the PDMS arms and the Py reporter molecule.

Figure 9A presents the temperature-dependent fluorescence anisotropy ($\lambda_{em} = 380 \pm 5$ nm) for Py-PDMS-Py in pure [C_4mim][Tf_2N] and [C_4mim][Tf_2N]/50% toluene. The solid lines that pass through the data are

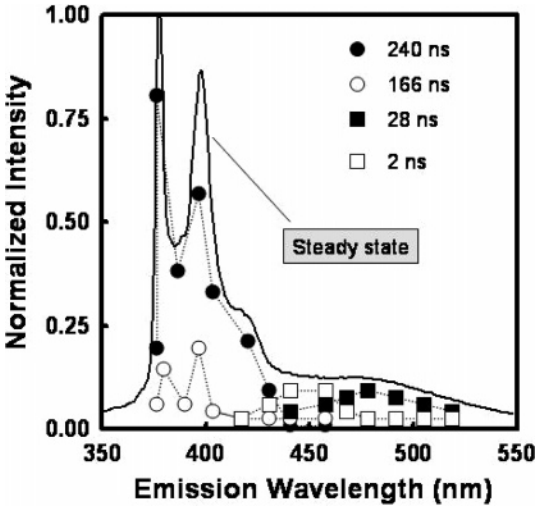

Figure 8. Decay associated spectra (DAS) for Py-PDMS-Py in [C_4mim][Tf_2N]/50% toluene at 293 K. The apparent lifetimes for the individual spectral features are given in the figure. The corresponding steady-state spectrum is also shown. The uncertainty in each DAS datum is smaller than the size of each point.

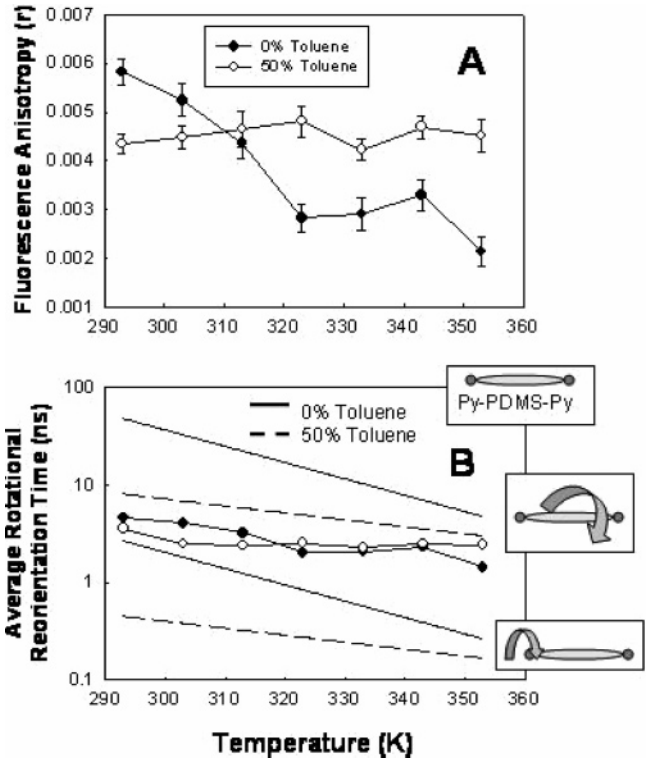

Figure 9. Temperature-dependent steady-state fluorescence anisotropy (panel A) and rotational reorientation times (panel B) for Py-PDMS-Py in pure [C_4mim][Tf_2N] (open symbols) and [C_4mim][Tf_2N]/50% toluene (closed symbols). In panel B are also shown predictions for the rotation reorientation times for intact Py-PDMS-Py molecules (upper set of curves) and the Py residue in isolated Py-PDMS-Py molecules (lower set of curves) in [C_4mim][Tf_2N] (—) and [C_4mim][Tf_2N]/50% toluene (- - -).

provided only to guide the reader's eye; they do not represent a model. There is a 3-fold decrease in Py-PDMS-Py steady-state fluorescence anisotropy in pure [C_4mim][Tf_2N] as temperature increases. This is consistent, in part, with the decrease in solvent viscosity (cf. Figure 4B). Interestingly, within our measurement precision, the steady-state fluorescence anisotropy is temperature-independent for Py-PDMS-Py in [C_4mim][Tf_2N]/50% toluene.

By using the average excited-state fluorescence lifetimes at each temperature and the Perrin equation (eq 4), we can estimate the rotational correlation times for Py-PDMS-Py. The temperature-dependent "Py-PDMS-Py" rotational correlation times in pure [C_4mim][Tf_2N] and [C_4mim][Tf_2N]/50% toluene are presented in Figure 9B. (Note: The *y*-axis in Figure 9B is logrithmic.) To predict the temperature-dependent behavior of isolated Py-PDMS-Py molecules in pure [C_4mim][Tf_2N] and [C_4mim][Tf_2N]/50% toluene, we used eq 5 or 6, respectively, to estimate the rotational reorientation time of the Py residue alone or a globular molecule with a molecular weight equal to the Py-PDMS-Py absolute molar mass ($M = 3100$ g/mol) and temperature-independent values for ν_s and s (i.e., $\nu_s = 1.03$ mL/g[27] and $s = 0$). The upper and lower solid curves in Figure 9B are the predictions in pure [C_4mim][Tf_2N] if the rotational reorientation dynamics were governed by the global motion from isolated Py-PDMS-Py molecules or the local motion from the Py residue on an isolated Py-PDMS-Py molecule, respectively. (Note: To estimate the steady-state anisotropy for a Py residue, we assumed a volume of an isolated pyrene molecule, 200−230 Å^3.[28]) The upper and lower dashed curves in Figure 9B are the estimates in [C_4mim][Tf_2N]/50% toluene if the rotational reorientation dynamics were governed by the global motion from an isolated Py-PDMS-Py molecule or the local motion from the Py residue on an isolated Py-PDMS-Py molecule, respectively.

Although steady-state anisotropy experiments have limitations,[29] and our assumptions preclude quantitative conclusions, differences between the experimental and estimated rotational correlation times can be used to qualitatively sense temperature- and composition-dependent changes in Py-PDMS-Py. For example, if we were forming rigid intermolecular aggregates (e.g., (Py-PDMS-Py)$_n$), one would expect the observed rotational correlation time to exceed the upper solid and dashed curves in Figure 9B. The experimental results are not consistent with this type of behavior. If the rotational dynamics were consistent with the Py residues moving independently of the PDMS segments, the observed rotational correlation times would follow the lower solid and dashed curves in Figure 9B. The experimental results are not consistent with this scenario. The overall behavior is consistent with Py residues and PDMS segments of individual Py-PDMS-Py molecules reorienting in a correlated manner. (Note: The behavior of Py-PDMS was equivalent to Py-PDMS-Py.)

Conclusions

We present the first results on the behavior of polymer tails in pure ionic liquids and ionic liquid/cosolvent mixtures. We report on the behavior of Py-PDMS-Py in [C_4mim][Tf_2N] as a function of added toluene (a good solvent for PDMS) and temperature. The Py-PDMS-Py dynamics are different in comparison to the behavior seen in good and Θ molecular solvents (toluene and ethyl acetate, respectively). The observed behavior is reminiscent, in part, of the behavior seen in a poor molecular solvent (methanol). The Py I_1/I_3 data suggest that the average Py residue is surrounded by a PDMS-rich microenvironment at all toluene loadings. We do not see any significant excimer-like emission in pure [C_4mim][Tf_2N] or [C_4mim][Tf_2N]/toluene mixtures

until we reach 50 vol % toluene. The Py-PDMS-Py ground state is heterogeneous, containing monomers and preformed excimer-like species prior to photoexcitation. The observed excimer-like emission does not arise from a classic dynamic excimer, or the rate of excimer formation is faster than our instrumental time resolution (≪2 ns). The Py-PDMS-Py time-resolved intensity decay data reveal that there are at least four emitting species in the IL phase. In the $[C_4mim][Tf_2N]$/50% toluene mixture at 293 K there are the following species in the IL phase: (i) a Py monomer in a PDMS-rich microenvironment, (ii) a Py monomer in a microenvironment between pure toluene and pure $[C_4mim][Tf_2N]$, (iii) a static ground-state dimer that has a geometry akin to a classical dynamically formed excimer, and (iv) a ground-state dimer that has the Py residues misaligned in comparison to (iii). Finally, steady-state anisotropy experiments are not consistent with the formation of rigid aggregates (i.e., $(\text{Py-PDMS-Py})_n$). The results are consistent with Py residues and PDMS segments of individual Py-PDMS-Py molecules reorienting in a correlated manner.

Acknowledgment. G.A.B. gratefully acknowledges LANL for providing generous support of this work in the form of both Director's and Frederick Reines Fellowships. F.V.B. acknowledges support from the United States Department of Energy.

References and Notes

(1) *Ionic Liquids in Synthesis*; Wasserscheid, P., Welton, T., Eds.; Wiley-VCH: Weinheim, 2003.
(2) *Green Industrial Applications of Ionic Liquids*; Rodgers, R. D., Seddon, K. R., Volkov, S., Eds.; NATO Sci. Ser. Vol. 92; Kluwer: Dordrecht, Netherlands, 2002.
(3) (a) Seddon, K. R. *J. Chem. Technol. Biotechnol.* **1997**, *68*, 351. (b) Welton, T. *Chem. Rev.* **1999**, *99*, 2071. (c) Brown, R. A.; Pollet, P.; McKoon, E.; Eckert, C. A.; Liotta, C. L.; Jessop, P. G. *J. Am. Chem. Soc.* **2001**, *123*, 1254. (d) Smietana, M.; Mioskowski, C. *Org. Lett.* **2001**, *3*, 1037. (e) Liu, F.; Abrams, M. B.; Baker, R. T.; Tumas, W. *Chem. Commun.* **2001**, *5*, 433. (f) Brennecke, J. F.; Maginn, E. J. *AIChE J.* **2002**, *47*, 2384. (g) Welton, T. *Coord. Chem. Rev.* **2004**, *248*, 2459. (h) Baker, G. A.; Baker, S. N.; Pandey, S.; Bright, F. V. *Analyst* **2005**, *130*, 800.
(4) Ma, H.-Y.; Wan, X.-H.; Chen, X.-F.; Zhou, Q.-F. *J. Polym. Sci., Part A* **2003**, *41*, 143.
(5) Hong, K.; Zhang, H.; Mays, J. W.; Vissar, A. E.; Brazel, C. S.; Holerby, J. D.; Reichert, W. M.; Rogers, R. D. *Chem. Commun.* **2002**, 1368.
(6) Vijayaraghavan, R.; MacFarlane, D. R. *Aust. J. Chem.* **2004**, *57*, 129.
(7) Vijayaraghavan, R.; MacFarlane, D. R. *Chem. Commun.* **2004**, 700.
(8) Vijayaraghavan, R.; Suroanarayanan, M.; MacFarlane, D. R. *Angew. Chem., Int Ed.* **2004**, *43*, 5363.
(9) (a) Kane, M. A.; Baker, G. A.; Pandey, S.; Maziarz III, E. P.; Hoth, D. C.; Bright, F. V. *J. Phys. Chem. B* **2000**, *104*, 8585. (b) Kane, M. A.; Pandey, S.; Baker, G. A.; Perez, S. A.; Bukowski, E. J.; Hoth, D. C.; Bright, F. V. *Macromolecules* **2001**, *34*, 6831. (c) Gardinier, W. E.; Kane, M. A.; Bright, F. V. *J. Phys. Chem. B* **2004**, *108*, 18520. (d) Gardinier, W. E.; Bright, F. V. *J. Phys. Chem. B* **2005**, *109*, in press.
(10) Baker, S. N.; Baker, G. A.; Bright, F. V. *Green Chem.* **2002**, *2*, 165.
(11) Baker, G. A.; Baker, S. N.; McCleskey, T. M. *Chem. Commun.* **2003**, 2932.
(12) (a) Birks, J. B. *Photophysics of Aromatic Molecules*; Wiley-Interscience: London, 1970; Chapter 7. (b) Winnik, M. A. *Acc. Chem. Res.* **1985**, *18*, 73. (c) *Photophysical and Photochemical Tools in Polymer Science*; Winnik, M. A., Ed.; D. Reidel Co.: Dordrecht, 1986.
(13) Beechem, J. M.; Gratton, E. In *Time-Resolved Laser Spectroscopy in Biochemistry;* Lakowicz, J. R., Ed.; SPIE: Bellingham, WA, 1988; Proc. SPIE 909, p 70.
(14) (a) Lakowicz, J. R. *Principles of Fluorescence Spectroscopy*, 2nd ed.; Kluwer Academic/Plenum Publishers: New York, 1999. (b) Steiner, R. F. In *Topics in Fluorescence Spectroscopy*; Lakowicz, J. R., Ed.; Plenum Press: New York, 1991; Vol. 3, pp 1−52. (c) Perrin, F. *J. Phys. Radium V, Ser. 6* **1926**, *7*, 390. (d) Perrin, F. *Ann. Phys. Ser. 10* **1929**, *12*, 169.
(15) (a) Berghmans, M.; Govaers, S.; Berghmans, H.; De Schryver, F. C. *Polym. Eng. Sci.* **1992**, *32*, 1466. (b) Morita, S.; Tsunomori, F.; Ushiki, H. *Eur. Polym. J.* **2002**, *38*, 1863. (c) Nichifor, M.; Lopes, S.; Bastos, M.; Lopes, A. *J. Phys. Chem. B* **2004**, *108*, 16463.
(16) (a) Waskiewicz, D. E.; Hammes, G. G. *Biochemistry* **1982**, *21*, 6489. (b) Liu, W.; Chen, Y.; Watrob, H.; Bartlett, S.; Jen-Jacobson, L.; Barkley, M. *Biochemistry* **1998**, *37*, 15457.
(17) Baker, S. N.; McCleskey, T. M.; Pandey, S.; Baker, G. A. *Chem. Commun.* **2004**, 940.
(18) Spencer, R. D.; Weber, G. *J. Chem. Phys.* **1970**, *52*, 1654.
(19) Thompson, R.; Gratton, E. *Anal. Chem.* **1988**, *60*, 670.
(20) (a) Riddick, J. A.; Bunger, W. B. *Organic Solvents*, 3rd ed.; Wiley-Interscience: New York, 1970. (b) Harris, K. R. *J. Chem. Eng. Data* **2000**, *45*, 893.
(21) (a) Wong, A. L.; Hunnicutt, M. L.; Harris, J. M. *Anal. Chem.* **1991**, *63*, 1076. (b) Karpovich, D. S.; Blanchard, G. J. *J. Phys. Chem.* **1995**, *99*, 3951.
(22) (a) Dong, D. C.; Winnik, M. *Photochem. Photobiol.* **1982**, *35*, 17. (b) Dong, D. C.; Winnik, M. A. *Can. J. Chem.* **1984**, *62*, 2560. (c) Waris, R.; Acree, Jr., W. E.; Street, Jr., K. W. *Analyst* **1988**, *113*, 1465.
(23) (a) Zagrobelny, J.; Betts, T.; Bright, F. *J. Am. Chem. Soc.* **1992**, *114*, 5249. (b) Winnik, F. *Chem. Rev.* **1993**, *93*, 587. (c) Rice, J. K.; Niemeyer, E. D.; Dunbar, R. A.; Bright, F. V. *J. Am. Chem. Soc.* **1995**, *117*, 5832.
(24) Redpath, A. E. C.; Winnik, M. A. *J. Am. Chem. Soc.* **1982**, *104*, 5604.
(25) (a) Badea, M. G.; Brand, L. *Methods Enzymol.* **1979**, *61*, 378. (b) Knutson, J. R.; Walbridge, D. G.; Brand, L. *Biochemistry* **1982**, *21*, 4671.
(26) (a) Yamazaki, T.; Tamai, N.; Yamazaki, I. *Chem. Phys. Lett.* **1986**, *124*, 326. (b) Yamazaki, I.; Tamai, N.; Yamazaki, T. *J. Phys. Chem.* **1987**, *91*, 3572. (c) Taniguchi, Y.; Mitsuya, M.; Tamai, N.; Yamazaki, I.; Masuhara, H. *Chem. Phys. Lett.* **1986**, *132*, 516. (d) Yamazaki, I.; Winnik, F. M.; Winnik, M. A.; Tazuke, S. *J. Phys. Chem.* **1987**, *91*, 4213. (e) Tsujii, Y.; Itoh, T.; Fukuda, T.; Miyamoto, T.; Ito, S.; Yamamoto, M. *Langmuir* **1992**, *8*, 936. (f) Declercq, D.; Delbeke, P.; De-Schryver, F. C.; VanMeervelt, L.; Miller, R. D. *J. Am. Chem. Soc.* **1993**, *115*, 5702. (g) Tsuchida, A.; Ikawa, T.; Tomie, T.; Yamamoto, M. *J. Phys. Chem.* **1995**, *99*, 8196. (h) Dutta, A. K.; Misra, T. N.; Pal, A. J. *Langmuir* **1996**, *12*, 459.
(27) *Silicon Compounds. Register and Review*, United Chemical Technologies, pp 254−255.
(28) Jiang, Y.; Blanchard, G. J. *J. Phys. Chem.* **1994**, *98*, 6436.
(29) In cases where a relatively small fluorescent probe is attached to a larger macromolecule, the observed steady-state fluorescence anisotropy from the probe results from a combination of local probe motion, segmental motion of a subregion of the entire macromolecule and the probe, and/or the global motion of the macromolecule. As a result, if there is local/segmental dynamics, which is likely here, the measured experimental steady-state fluorescence anisotropy is biased toward lower values in comparison to what the value would be if the probe did not undergo local/segmental motion. Thus, the steady-state anisotropy measurements tend to underestimate intermolecular association if the associating species are flexible, and the probe can undergo motion independent of the macromolecule.

MA051313N